BMC Medical Imaging

RESEARCH

Open Access

Correlation of sonographic features with prognostic factors in ductal carcinoma in situ of the breast: an exploratory study using ultrasound and shear wave elastography

Jianan Shi[1,2†], Shiyun Yang[1†], Qinghua Niu[1], Lei Zhao[1], Chao Jia[1], Lianfang Du[1], Fan Li[1*] and Yang Liu[1*]

Abstract

Objective Ductal carcinoma in situ (DCIS) of the breast has a wide disease spectrum with risks of progression to invasive cancer linked to pathological factors. High-grade histology, large tumor volume, and comedonecrosis are adverse prognostic factors. This study explores the correlation between conventional ultrasound (Con-US) and shears wave elastography (SWE) features with DCIS prognostic factors and evaluates their predictive efficacy.

Methods A retrospective analysis was conducted on clinical data, Con-US, and SWE imaging features of 83 DCIS patients who underwent surgical resection between June 2018 and December 2022. Binary logistic regression analysis was performed to explore the relationship between sonogram indices and pathological prognostic factors.

Results The results revealed that microcalcification observed on Con-US was an independent risk factor for high-grade DCIS and comedonecrosis [odds ratio (OR): 5.316 and 4.512]. In SWE analysis, the Emax value was significantly different between the non-high-grade and high-grade DCIS groups($P=0.006$), with an Emax value greater than 75.03 kPa identified as an independent risk factor for high-grade DCIS [OR:1.022, the area under the curve (AUC): 0.682, 95% confidence interval (CI): 0.555–0.808]. Additionally, the Ecolor, Emax, Emean, and Emean SD values were statistically different between the groups with and without comedonecrosis ($P=0.049$, 0.006, 0.012, 0.022), with an Emean value exceeding 30.45 kPa identified as an independent risk factor for comedonecrosis (OR:1.025, AUC:0.708, 95% CI:0.562–0.854). Furthermore, combining microcalcification on Con-US with specific SWE indicators demonstrated an improved predictive specificity for high-grade DCIS and comedonecrosis (0.902 and 0.889, respectively). No significant difference was found in other indexes on SWE.

†Jianan Shi and Shiyun Yang contributed equally to this work.

*Correspondence:
Fan Li
medicineli@sjtu.edu.cn
Yang Liu
liuyangshsmu@163.com

Full list of author information is available at the end of the article

Conclusions The microcalcification signs on Con-US, Emax and Emean values on SWE analysis are associated with the high nuclear grade and comedonecrosis of DCIS, the combination of Con-US and SWE can improve the predictive specificity of DCIS-related prognostic factors.

Keywords Ductal carcinoma in situ, Conventional ultrasound, Shear wave elastography, Prognostic factors, Nuclear grade, Comedonecrosis

Introduction

Ductal carcinoma in situ (DCIS) is a tumor formed by abnormal proliferation of epithelial cells in the ductallobular unit of the breast; however, it does not invade the basement membrane. The characteristics of DCIS include active epithelial cell proliferation, abnormal cell morphology, and necrosis. The degree of malignancy and the prognosis of DCIS after treatment are related to the nuclear grading of the tumor, histopathological and structural features, presence of comedonecrosis, and expression of various molecular biomarkers. High-grade DCIS is associated with rapid growth and early infiltration, while low-grade DCIS shows inert clinical behavior, grows slowly, and has morphological and biological features similar to atypical hyperplasia [1, 2]. In addition to nuclear grading, the presence of tumor-associated comedonecrosis and microcalcifications has been associated with increased invasiveness of DCIS and the risk of local recurrence after conservative treatment. Molecular biomarkers associated with the prognosis of invasive breast cancer include the estrogen receptor (ER), progesterone receptor (PR), human epidermal growth factor receptor 2 (HER2), and Ki-67 proliferation index. Recent studies have shown that DCIS with high expression of HER2 has a poor prognosis [3], while the Ki-67 index is positively correlated with DCIS recurrence [4].

It is based on the high degree of heterogeneity of DCIS in terms of histological morphology and biological features, with wide variation in imaging manifestations. Mammography, magnetic resonance imaging (MRI), and ultrasound (US) are commonly used imaging methods for the diagnosis of breast disease. MRI has high soft-tissue resolution and its diagnostic sensitivity for DCIS varies, with a meta-analysis showing that its sensitivity ranges from 40 to 100%, which is related to the differentiated distribution of neovascularization within the lesion and the setting of technical parameters [5]. Mammography is considered the preferred method of breast imaging diagnosis in Europe and the United States; it has the characteristics of standardization, high efficiency, and high detection rate of calcification. Although molybdenum targets are the main method of detecting DCIS in conventional imaging, they are not ideal for showing mass-type lesions, noncalcified lesions, and dense breasts. Although US is somewhat subjective, a growing number of studies in recent years have shown that US has advantages in the examination of dense breasts and shows good results in DCIS without microcalcifications. Furthermore, early studies have shown a correlation between DCIS characteristics in US imaging and its prognostic factors. For example, high-grade DCIS usually shows ductal changes with microcalcifications on US images, while intermediate- or low-grade DCIS shows hypoechoic masses with microfollicularity, irregular morphology, and fuzzy borders [6–8]. ER-positive expression is correlated with mass-like DCIS, while ER-negative DCIS is more likely to be detected on US images than ER-positive DCIS, which has larger lesions and is usually accompanied by posterior acoustic shadowing [8].

In recent years, elastography, a real-time noninvasive imaging technique, has been shown to sensitively detect the texture hardness of lesions and has been included in the fifth edition of the BI-RADS guidelines for the diagnosis of breast masses. Among multiple elastography techniques, shear wave elastography (SWE) has better examination consistency and greater reproducibility and can be quantitatively analyzed, providing greater advantages in clinical practice. Previous studies [9] applying SWE in invasive ductal carcinoma (IDC) have found that SWE hardness values are associated with nuclear grade, extent of tumor infiltration, lymph node metastasis, tumor type, and vascular invasion can predict whether DCIS is accompanied by invasive carcinoma. There have been limited reports on the elastography characteristics of DCIS. Leong LC et al. [10] had earlier shown that strain elastography could correlate with the type of DCIS histological architecture but it did not demonstrate a definite association with DCIS nuclear grade. In this study, our objective was to comprehensively analyze the imaging characteristics of DCIS using both conventional US (Con-US) and SWE. We employed qualitative and quantitative indices to investigate potential predictive factors for DCIS and their correlation with prognostic indicators.

Materials and methods

Patients

Patients hospitalized for breast lesions were recruited between June 2018 and December 2022. The inclusion criteria were as follows: (1) patients with pathologically

confirmed DCIS by surgical resection; (2) postoperative pathology data containing complete information on pathological prognostic factors; (3) complete clinical information; (4) complete Con-US and SWE images of good quality; (5) surgery performed within a month after the US examination; (6) no treatment before the US examination. Any cases that did not meet one of the above criteria were excluded.

This retrospective study was approved by the Ethics Committee of the Hospital, and the requirement for patient approval or informed consent was waived.

Con-US and elastography examination

Aplio500 (CANON, Japan) and Aplio i900 (CANON, Japan) color Doppler diagnostic instruments were used. The probes were 14–5 L and 14–8 L, and the frequencies were 5–14 MHZ and 8–14 MHZ, respectively. A complete US scan of the breasts revealed and stored grayscale and color Doppler flow images or Power Doppler flow images of the long- and short-axis sections of the lesion. After acquisition of Con-US, the largest plane of the lesion was selected to fix the probe, and the dual-amplitude mode was used to perform the SWE examination of the lesion. The depth was set within 4 cm, and the range of the color scale was 0–55 kPa. The US probe was placed gently on the surface of the breast to avoid applying too much pressure on the skin and to ensure that the lesion and its surrounding normal breast tissues were within the sampling frame. In the sample frame, the lesion was located in the center of the screen, with a continuous acquisition time of 3–5 s. Images were frozen and stored after the color was filled completely, and the operation was repeated three times, from blue to green to orange to red, which indicated a gradual increase in the hardness of the lesion. All US examinations were performed by a senior radiologist with 20 years of experience.

Image analysis

In Con-US, the morphology was divided into mass lesion (ML) and non-mass lesion (NML), according to previous studies [6]. The presence or absence of microcalcifications, the blood flow signal (abundant/non-abundant or absent) on Color Doppler flow imaging (CDFI)and BI-RADS classification were recorded. The indicators on SWE image were included: (1) color pattern (mainly blue/green and mainly orange/red) [11]; (2) uniformity of distribution (uniform/underuniform and nonuniform) [11]; (3) Emax, acquired within the region of interest, is configured as a circular area with a diameter of 2–3 mm. This area is positioned on the firmest section and the vicinity of the lesions to capture the highest elasticity value. (4) Emean and Emean SD were obtained by delineating the region of interest along the borders of the lesions. The images were captured three times and analyzed to calculate the average elasticity value and standard deviation. All evaluations were conducted by two senior radiologists who performed elastography quantitative analysis without access to the pathological results. The agreement between the radiologists in assessing Con-US and SWE images was measured using weighted kappa (κ) to evaluate inter-observer agreement.

Pathological results analysis

The pathological analysis indicators for this study were the following: (1) according to nuclear grade, DCIS was divided into three grades: low, intermediate, and high [12]; (2) the histological pathological maximum diameter of the tumors was recorded; and (3) the immunohistochemical results were strictly determined according to the kit instructions. ER-, PR-, and Ki-67-positive cells produce brown granules in the nucleus. The cut-off point for ER and PR positive is ≥10% [13], and the cut-off point for Ki-67 positive is ≥20% [14]. C-erbB2 (+) cells produce brown granules in the cell membrane or cytoplasm. C-erbB2 (+++), patients with confirmed C-erbB2 (++), and data that did not undergo Fisher's exact test were excluded [15]; (4) the presence of comedonecrosis [16].

Statistical analysis

We used SPSS 21 (IBM, USA) software to perform the statistical analysis. The measurement data (age) was presented as mean ± standard deviation. The parametric test (unpaired t-test) was used to compare the two groups. The other measurement data (Emax, Emean, and Emean SD) were presented as median values (interquartile range). Non-parametric tests were used for between-group comparison. Enumeration data were presented as a proportion (%) and used the χ [2] test or Fisher's exact test for comparison between groups. The weighted kappa was used to assess inter-observer agreement. Binary logistic regression analysis was used to analyze the correlations of pathological prognostic factors with Con-US and SWE imaging features and calculate the odds ratio (OR), 95% confidence interval (CI), and area under the curve (AUC). The receiver operating characteristic curve was used to evaluate the diagnostic value of different modalities and the value of joint analysis, and the Delong test was used to test the significance of different modalities. Statistical significance was set at $p < 0.05$.

Results

Clinical data

According to the inclusion criteria, 83 DCIS lesions in 83 patients were enrolled according to the inclusion criteria (Fig. 1). The age of the patients ranged from 33 to 81 years (average, 54.2 ± 11.0 years). Patient characteristics, mass size, immunomarkers (+/-), and pathological grades are shown in Table 1.

DCIS between groups with different prognostic factors on Con-US and SWE sonograms

On Con-US images, microcalcifications showed statistically significant differences between the non-high-grade (low-grade and intermediate-grade) and high-grade DCIS groups, between the groups with and without comedonecrosis, between the PR(+)/(-) group, and between the HER2(+)/(-) group ($p = 0.000$, 0.002, 0.022, and 0.014 respectively).The morphology of the lesions (NML/ML) showed a statistically significant difference between the non-high-grade and high-grade DCIS groups ($p = 0.030$). BI-RADS classification (3-4a/≥4b) was statistically different between the non-high-grade and high-grade DCIS groups, the group with or without comedonecrosis, the group with or without microinfiltration, and the HER2(+)/(-) group ($p = 0.000$, 0.000, 0.048, and 0.019, respectively), and CDFI blood flow signal did not show statistically significant differences between all prognostic factor groups (Table 2).

In the SWE images (Figs. 2, 3 and 4), the Emax values were significantly different between the non-high-grade and high-grade DCIS groups and the group with and without comedonecrosis ($p = 0.006$ and 0.006, respectively). The Ecolor, Emean values, and EmeanSD values were statistically significant between the groups with and without comedonecrosis ($p = 0.049$, 0.012, and 0.022, respectively), Ehomo was statistically different between the groups with and without microinfiltration ($p = 0.029$). The sonographic indices of SWE did not show statistically significant differences between the groups of each immunomarker (Table 3).

Independent predictors and predictive efficacy in Con-US and SWE images

According to binary logistic regression analysis, microcalcification was an independent risk factor for high-grade DCIS and comedonecrosis on Con-US images, with relative risks (OR) of 5.316

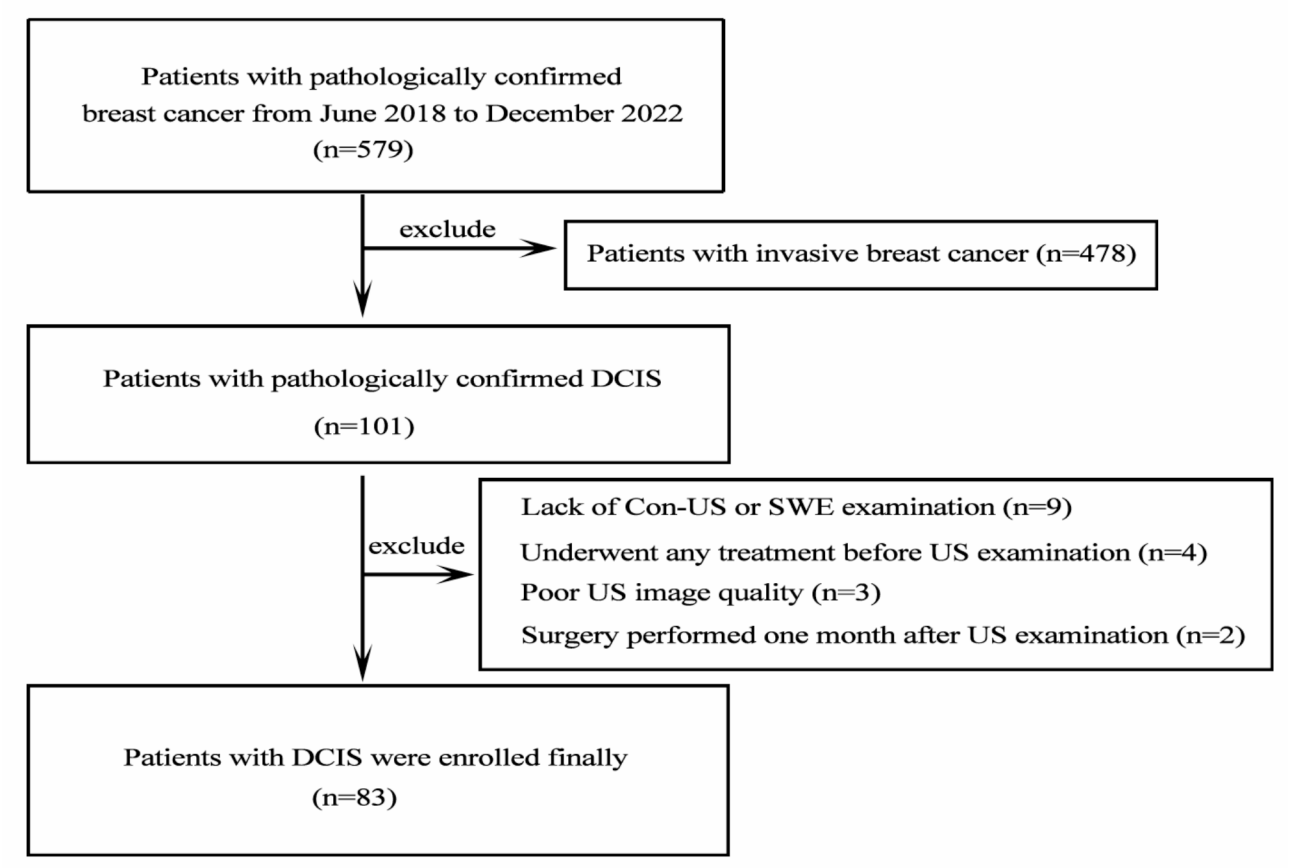

Fig. 1 Flow chart for patient inclusion

Table 1 Clinical information for 83 patients with ductal carcinoma in situ

Characteristics		*n* (%)
Age		
	≥ 50 y	51 (61.4)
	< 50 y	32 (38.6)
Symptom		
	Mass	65 (78.3)
	Bleeding	2 (2.4)
	Pain	5 (6.0)
	Asymptomatic	11 (13.3)
Pathological diameter		
	≥ 2 cm	30 (36.1)
	< 2 cm	53 (63.9)
Comedonecrosis		
	Yes	35 (42.2)
	No	48 (57.8)
ER		
	Positive	53 (63.9)
	Negative	30 (36.1)
PR		
	Positive	34 (41.0)
	Negative	49 (59.0)
Ki-67		
	Positive	30 (36.1)
	Negative	53 (63.9)
HER2		
	Positive	21 (25.3)
	Negative	62 (74.7)
Microinvasion		
	Yes	29 (34.9)
	No	54 (65.1)
Lymph nodes metastasis		
	Yes	1 (1.2)
	No	82 (98.8)

Data are presented as *n* (%)

ER, estrogen receptor; PR, progesterone receptor; HER2, human epidermal growth factor receptor 2

and 4.512, respectively. The corresponding AUCs were 0.699 (95% CI: 0.578–0.819) and 0.678 (95% CI, 0.523–0.833). On SWE analysis, Emax > 75.03 kPa was an independent risk factor for high-grade DCIS with an OR of 1.022 and an AUC of 0.682 (95% CI, 0.555–0.808). Emean > 30.45 kPa was an independent risk factor for comedonecrosis, with an OR of 1.025 and an AUC of 0.708 (95% CI, 0.562–0.854), and microcalcification indices in Con-US in combination with Emax > 75.03 kPa and Emean > 30.45 kPa improved the predictive specificity of high grade and comedonecrosis over the use of indices alone by 0.902 and 0.889, respectively (Table 4).

Inter-observer reproducibility

For evaluating the Con-US and SWE images, two senior radiologists showed substantial agreement (κ = 0.879; 95%CI, 0.826–0.923 and κ = 0.921; 95%CI, 0.852– 0.990, respectively).

Discussion

With the gradual deepening of the understanding of DCIS US sonograms, Con-US sonogram features have been shown to correlate with prognostic factors of DCIS, showing the feasibility of prognostic prediction of DCIS from a US imaging perspective. A previous study has shown [17] that microcalcifications in grayscale US are valid indicators of an increased risk of malignancy in patients with DCIS. The present study showed similar findings and confirmed that microcalcifications are independent risk factors for predicting high-grade DCIS and comedonecrosis. Although blood flow signals, lesion morphology, and BI-RADS classification were included, these signs were not independent risk predictors.

Elastography is a new US diagnostic technique based on non-invasive evaluation of tissue mechanical properties. Although there are various elastography techniques, SWE is more widely used in clinical practice due to its ability to objectively obtain lesion hardness values (e.g., Emax value, Emean value, and Emin value), as well as the advantages of higher accuracy and reproducibility. One advantage of this method is that it is widely used in clinical practice. Due to the rapid progression of malignant tumors, there is an increase in the number of tumor stromal cells, collagen fibers, and remodeling, increasing the hardness of the tissue. Based on this pathophysiological alteration, SWE technology has great potential for the identification and prediction of malignant breast lesions. Preliminary studies have shown the correlation between SWE quantitative indices and prognostic factors in IDC of the breast; however, there are few results in DCIS. In this study, qualitative and quantitative elasticity indicators were included, and the results showed that only the quantitative indicator, the Emax value, was correlated with the pathological grading of DCIS. Previous studies showed that Emax has been confirmed as an auxiliary method for distinguishing between benign and malignant breast masses (esp. IDC) and predicting the risk of invasiveness of DCIS. However, there are differences in the cutoff values, which may be related to the use of different instruments, types of included cases, the size of the lesion and BI-RADS classifications. Previous studies have shown that the cutoff value for diagnosing IDC obtained using the SuperSonic series instrument is higher (range from 80 to 180 kPa) [11, 18, 19]. Chang JM et al. [20] found

Table 2 Image characteristics and immunomarker characteristics of ductal carcinoma in situ on conventional ultrasound n(%)

Parameters	US pattern		*p*	Microcalcification		*p*	Vascularization on CDFI		*p*	BI-RADS category		*p*
	mass-like (*n* = 41)	non-mass-like (*n* = 42)		Presence (*n* = 29)	Absence (*n* = 54)		No/poor (*n* = 45)	Rich (*n* = 38)		3–4a (*n* = 38)	≥ 4b (*n* = 45)	
Pathological grade			**0.030***			**0.000***			0.129			**0.000***
Non-high-grade	30(73.2)	21(50.0)		10(34.5)	41(75.9)		31(68.9)	20(52.6)		32(84.2)	19(42.2)	
High-grade	11(26.8)	21(50.0)		19(65.5)	13(24.1)		14(31.1)	18(47.4)		6(15.8)	26(57.8)	
Comedonecrosis			0.144			**0.002***			0.076			**0.000***
Yes	14(34.1)	21(50.0)		19(65.5)	16(29.6)		15(33.3)	20(52.6)		5(13.2)	30(66.7)	
No	27(65.9)	21(50.0)		10(34.5)	38(70.4)		30(66.7)	18(47.4)		33(86.8)	15(33.3)	
Microinvasion			0.126			0.367			0.898			**0.048***
Yes	11(26.8)	18(42.9)		12(41.4)	17(31.5)		16(35.6)	13(34.2)		9(23.7)	20(44.4)	
No	30(73.2)	24(57.1)		17(58.6)	37(68.5)		29(64.4)	25(65.8)		29(76.3)	25(55.6)	
ER			0.708			0.092			0.736			0.087
Positive	27(65.9)	26(61.9)		15(51.7)	38(70.4)		28(62.2)	25(65.8)		28(73.7)	25(55.6)	
Negative	14(34.1)	16(38.1)		14(48.3)	16(29.6)		17(37.8)	13(34.2)		10(26.3)	20(44.4)	
PR			0.325			**0.022***			0.846			0.124
Positive	19(46.3)	15(46.9)		7(24.1)	27(50.0)		18(40.0)	16(42.1)		19(50.0)	15(33.3)	
Negative	22(53.7)	17(53.1)		22(75.9)	27(50.0)		27(60.0)	22(57.9)		19(50.0)	30(66.7)	
HER2			0.488			**0.014***			0.845			**0.019***
Positive	9(22.0)	12(28.6)		12(41.4)	9(16.7)		11(24.4)	10(26.3)		5(13.2)	16(35.6)	
Negative	32(78.0)	30(71.4)		17(58.6)	45(83.3)		34(75.6)	28(73.7)		33(86.8)	29(64.4)	
Ki-67			0.406			0.092			0.903			0.210
Positive	13(31.7)	17(40.5)		14(48.3)	16(29.6)		16(35.6)	14(36.8)		11(28.9)	19(42.2)	
Negative	28(68.3)	25(59.5)		15(51.7)	38(70.4)		29(64.4)	24(63.2)		27(71.1)	26(57.8)	

*Statistically significant difference

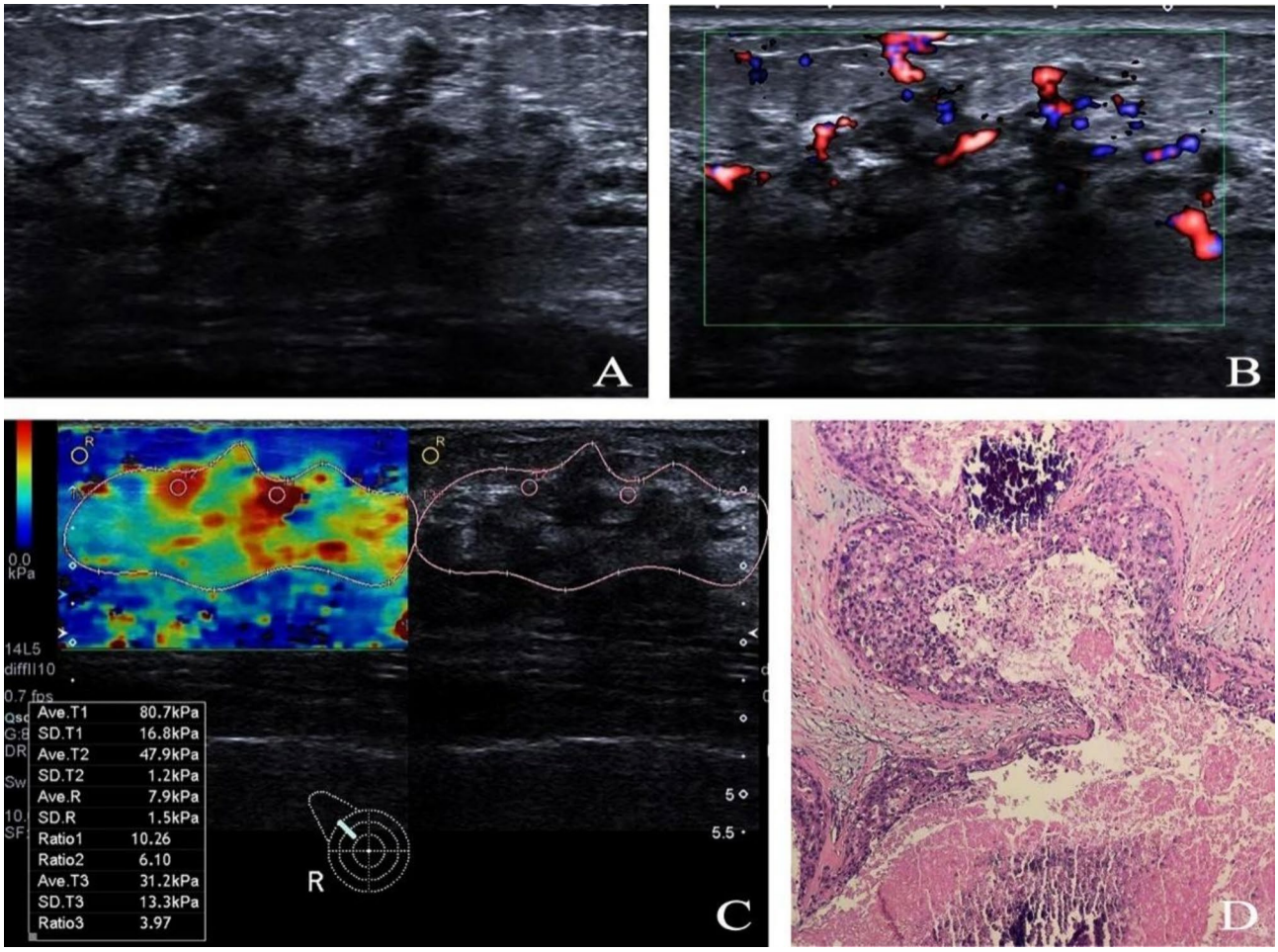

Fig. 2 (**A**) Conventional ultrasound shows a non-mass lesion without microcalcifications in the right mammary outer upper quadrant, BI-RADS 4a. (**B**) Color Doppler shows a rich blood flow signal in the lesion. (**C**) Shear wave elastography dual-screen image (left shear wave elastographyimage, right corresponding grayscale image) and measuring quantitative parameters, Emax for 64.3 kPa, and Emean for 31.2 kPa. (**D**) The case confirmed mid-grade ductal carcinoma in situ with comedonecrosis

that the Young's modulus values for invasive cancer (including ductal carcinoma and lobular carcinoma) were higher than those for ductal carcinoma in situ when using SuperSonic SWE imaging (157.5±57.07 and 169.5±61.06 vs. 117.8 kPa±54.72). Evans A [9] and Bae JS [21] also used SuperSonic to establish cutoff values of Emean greater than 50 kPa and 70.7 kPa respectively as determining factors for predicting whether DCIS is associated with invasive components. The cutoff value range for diagnosing IDC using the Canon series instrument is 50.85 kPa to 86.45 kPa [22, 23], which is lower than the SuperSonic series. In this study, the Canon 500 and i900 were used for detection, and the threshold for high-grade DCIS at 75.03 kPa falls within the previously reported range for IDC.

Research exploring the use of SWE for prognostic prediction in invasive breast cancers has unveiled significant correlations with key factors such as pathological nuclear grade and tumor infiltration. Evans et al. [9, 24, 25] highlighted the positive association of the Emean value with these factors. In a similar vein, Kim et al. [22] emphasized the importance of a high EmeanSD value. Notably, while studies on DCIS prognosis and SWE indices are scarce, and this study is the first to explore and reveal the relationships between these factors. Our findings illuminate the strong link between a high Emax value and tumor differentiation, with Emax > 75.03 kPa identified as a compelling independent risk factor for predicting high-grade DCIS prognosis after thorough logistic regression analysis.

Comedonecrosis is an important factor in the poor prognosis of DCIS and is associated with increased tumor cell proliferative activity [26] and clinically aggressive behavior [27]. The pathological basis of comedonecrosis is the formation of necrotic areas due to hypoxia in the center of the cancerous lesion, which usually forms casting-type, coarse, or fine linear microcalcifications and can be identified by

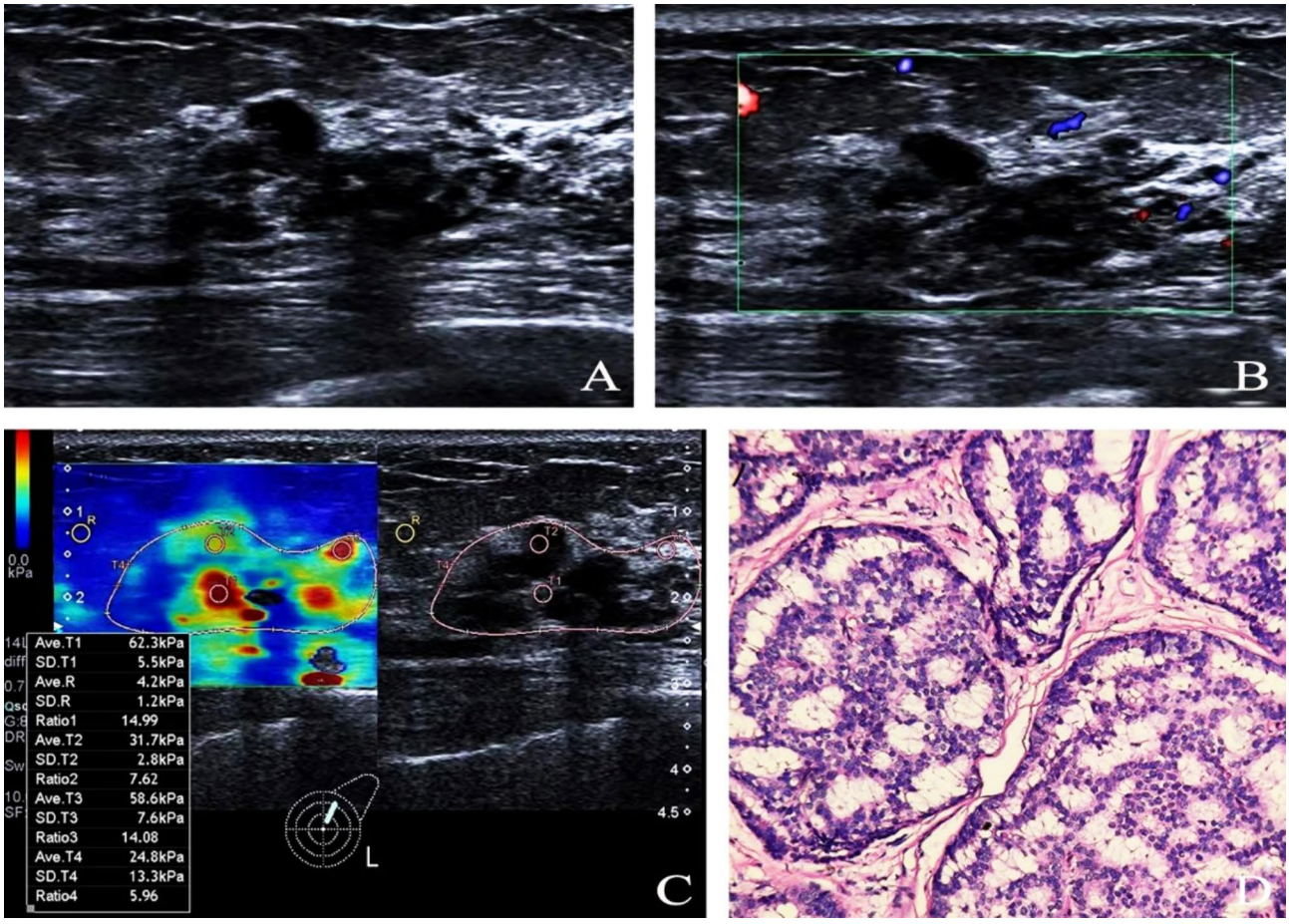

Fig. 3 (**A**) Conventional ultrasound shows a mass lesion without microcalcifications in the left mammary outer upper quadrant, BI-RADS 4b. (**B**) Color Doppler shows a small blood flow signal in the lesion. (**C**) Shear wave elastography dual screen image (left shear wave elastography image, right corresponding grayscale image) and measuring quantitative parameters, Emax for 50.9 kPa, and Emean for 24.8 kPa. (**D**) Case confirmed mid-grade ductal carcinoma in situ without comedonecrosis

molybdenum targeting and US [28, 29]. In this study, we found that Ecolor, Emax, Emean, and EmeanSD were significantly different between groups with and without concomitant comedonecrosis, indicating that DCIS tumors with concomitant comedonecrosis showed a significant increase in hardness and heterogeneity on sonograms. After logistic regression analysis, only Emean > 30.45 kPa was found to be an independent factor for comedonecrosis, which is based on the mean value derived from enveloping the entire lesion. This better reflects the in-homogeneity within the tumor, which increases when there are areas of active proliferation, hypoxia, and necrosis within the tumor. High-grade DCIS, commonly associated with comedonecrosis, may explain the increased hardness observed. The presence of central comedonecrosis in high-grade DCIS contributes to the elevated stiffness and hardness compared to low-grade tumors. This necrotic material within the ductal lumens results in a denser and firmer texture, accentuating the stiffness characteristic of high-grade DCIS tumors [30]. Our findings indicate that regions of increased stiffness are predominantly located in the superficial layers of the lesion, raising the possibility that desmoplasia may contribute to this observation. Although desmoplasia is typically associated with invasive cancers, it is less frequently discussed in the context of DCIS. However, some studies suggest that DCIS with comedonecrosis may exhibit stromal changes resembling early desmoplastic reactions, likely due to the biological aggressiveness of high-grade DCIS and its interaction with the surrounding microenvironment [31].

In this study, we compared sonographic differences between different molecular biomarkers, including ER-, PR-, HER2, and Ki-67 negative and positive groups, and the results cannot identify a valid independent predictor.

This study has some limitations. Firstly, being a retrospective study with a limited sample size, potential selection bias may exist. Given the low incidence of

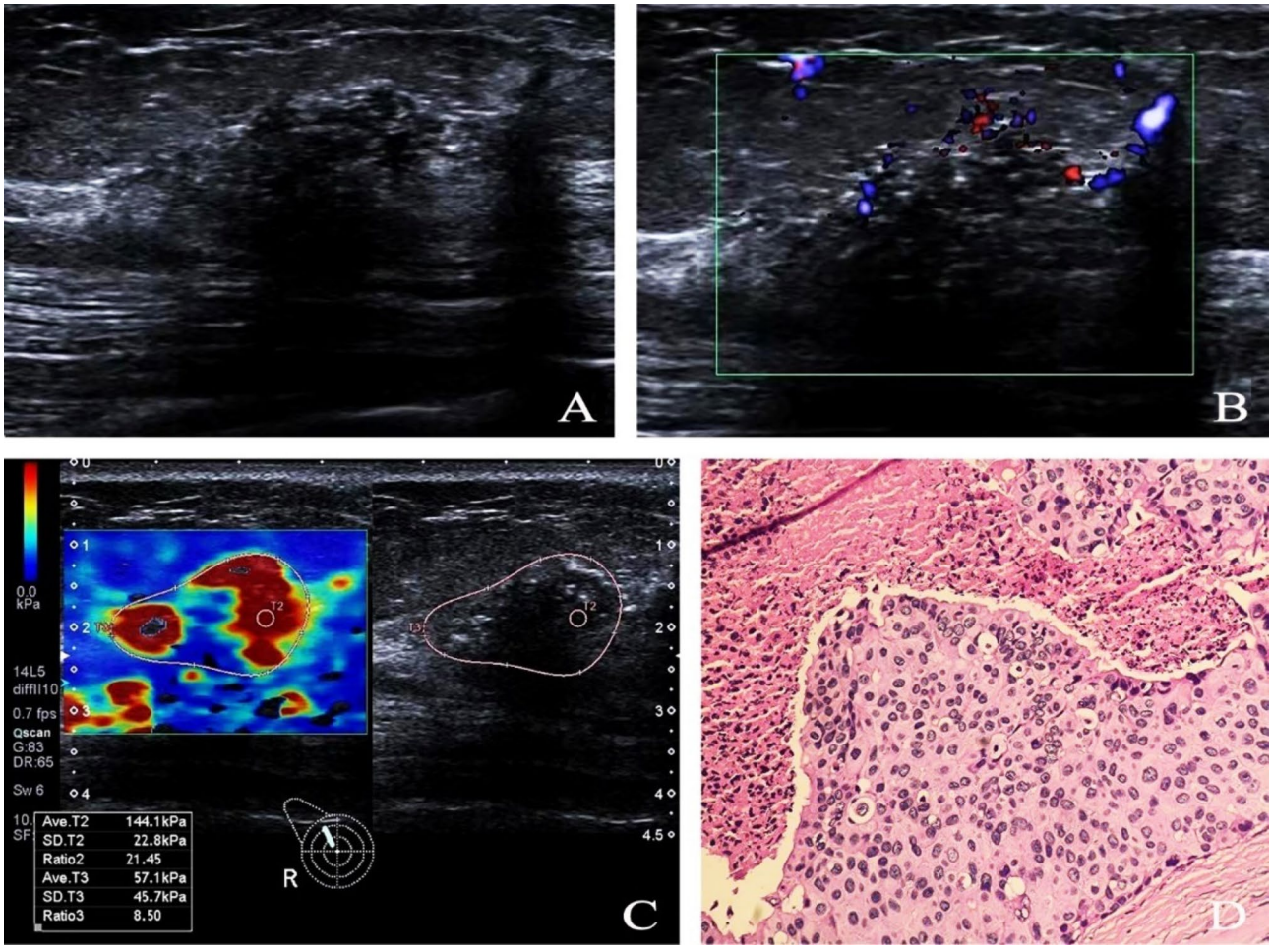

Fig. 4 (**A**) Conventional ultrasound shows a non-mass lesion with multiple microcalcifications in the right mammary outer upper quadrant, BI-RADS 4b. (**B**) Color Doppler shows a rich blood flow signal in the lesion. (**C**) Shear wave elastography dual-screen image (left shear wave elastography image, right corresponding grayscale image) and measuring quantitative parameters, Emax for 144.1 kPa, and Emean for 57.1 kPa.; (**D**) The case confirmed high-grade ductal carcinoma in situ with comedonecrosis and microinfiltration

DCIS and the study's single-center nature, the number of cases is relatively inadequate. To address this, we aim to conduct a multi-center prospective study in the future to enhance case collection. Second, this study was conducted in a single center, and due to the high variability of DCIS US images, different physicians may have different opinions; thus, a multicenter study under uniform criteria is needed. Third, DCIS associated with microinvasion (DCIS-MI) was included in this study, which has imaging features similar to those of pure DCIS on US images. This study only found Ehomo differences between groups and did not find an independent predictor of risk indicators for DCIS-MI. Previous studies have reported that blood flow richness is an independent risk factor for predicting DCIS-MI. Considering the differences in color Doppler display performance and influencing factors, this study found that pure DCIS also showed blood flow richness, and the ability to accurately predict DCIS-MI needs to be further investigated by expanding the sample size.

Conclusions

Microcalcification signs on Con-US and SWE sonographic Emax and Emean metrics were effective in predicting high-grade DCIS and DCIS with comedonecrosis, and the combination of the two helped improve the specificity of prediction.

Table 3 Ductal carcinoma in situ image characteristics and immune marker characteristics on shear wave elastography n(%)

Parameters	Ecolor		*p*	Ehomo		*p*	Emax M(IQR)	*p*	Emean M(IQR)	*p*	EmeanSD M(IQR)	*p*
	Blue/Green (*n* = 29)	Orange/ Red (*n* = 54)		Homo- (*n* = 10)	Reason- ably homo-/ hetero-(*n* = 63)							
Pathological			0.132			0.173		**0.006***		0.396		0.056
Non-high grade	21(72.4)	30(55.6)		4(40.0)	47(74.6)		45.6 (45.5)		27.1 (30.4)		10.3 (13.0)	
High-grade	8(27.6)	24(44.4)		6(60.0)	26(25.4)		82.2 (72.1)		33.1 (43.2)		22.3 (35.3)	
Comedonecrosis			**0.049***			1.000		**0.006***		**0.012***		**0.022***
Yes	8(27.6)	27(50.0)		4(40.0)	31(42.5)		75.2 (54.0)		51.4 (48.4)		22.3 (24.4)	
No	21(72.4)	27(50.0)		6(60.0)	42(57.5)		42.5 (51.6)		23.3 (30.0)		8.6 (12.4)	
Microinvasion			0.949			**0.029***		0.603		0.918		0.462
Yes	10(34.5)	19(35.2)		7(70.0)	22(30.1)		69.4 (66.6)		31.9 (40.9)		13.7 (20.1)	
No	19(65.5)	35(64.8)		3(30.0)	51(69.9)		56.5 (66.3)		28.5 (36.1)		11.1 (24.7)	
ER			0.234			0.741		0.140		0.091		0.177
Positive	21(72.4)	32(59.3)		7(70.0)	46(63.0)		51.6 (57.7)		26.3 (25.0)		10.5 (11.8)	
Negative	8(27.6)	22(40.7)		3(30.0)	27(37.0)		67.0 (78.0)		51.7 (58.2)		20.4 (27.8)	
PR			0.114			0.733		0.261		0.495		0.245
Positive	15(51.7)	19(35.2)		5(50.0)	29(39.7)		51.0 (57.2)		26.3 (29.0)		10.5 (11.4)	
Negative	14(48.3)	35(64.8)		5(50.0)	44(60.3)		66.1 70.4)		31.9 (42.5)		17.6 (28.5)	
HER2			0.479			0.708		0.269		0.584		0.235
Positive	6(20.7)	15(27.8)		3(30.0)	18(24.7)		75.0 (82.8)		43.3 (43.2)		20.4 (28.8)	
Negative	23(79.3)	39(72.2)		7(70.0)	55(75.3)		60.4 (58.6)		28.8 (33.8)		11.1 (13.1)	
Ki-67			0.804			0.484		0.827		0.637		0.690
Positive	11(37.9)	19(35.2)		5(50.0)	25(34.2)		64.7 (65.0)		26.4 (36.5)		10.5 (17.3)	
Negative	18(62.1)	35(64.8)		5(50.0)	48(65.8)		63.0 (68.8)		38.0 (38.3)		12.7 (24.6)	

* Statistically significant difference

Table 4 Binary logistic regression analysis and predictive efficacy of the characteristics and pathological prognostic factors of conventional ultrasound and shear wave elastography images

Parameters	B	OR (95% CI)	*p*	Sensitivity	Specificity	AUC (95% CI)
High-grade						
Microcalcification on US	1.671	5.316 (1.944–14.538)	0.001	0.594	0.804	0.699 (0.578–0.819)
Emax value > 75.03 kPa	0.021	1.022 (1.007–1.036)	0.003	0.594	0.784	0.682 (0.555–0.808)
Both sides join forces			0.000	0.500	0.902*	0.755 (0.635–0.875)
Comedonecrosis						
Microcalcification on US	1.507	4.512 (1.723–11.822)	0.002	0.579	0.778	0.678 (0.523–0.833)
Emean value > 30.45 kPa	0.025	1.025 (1.003–1.048)	0.029	0.737	0.639	0.708 (0.562–0.854)
Both sides join forces			0.005	0.474	0.889*	0.734 (0.586–0.882)

The * showed that the both sides join is significantly higher thanalone($p<0.05$)

Acknowledgements
Not applicable.

Author contributions
Writing–Original Draft Preparation, JNS and SYY; Methodology and Funding Acquisition, FL and YL; administration, QHN and LZ; Writing–Review and Editing, CJ and LFD. All authors reviewed the manuscript.

Funding
This research was granted by the National Natural Science Foundation of China (Nos. 82202172 and 82272012). The funding bodies played no role in the design of the study and collection, analysis, and interpretation of data and in writing the manuscript.

Data availability
Data is provided within the manuscript file.

Declarations

Clinical trial number
Not applicable.

Ethics approval and consent to participate
The study was approved by institutional ethics board of Shanghai General Hospital (No. 2016KY221) and individual informed consent for this retrospective analysis was waived. All experiments were performed in accordance with relevant guidelines and regulations.

Competing interests
The authors declare no competing interests.

Author details
[1]Department of Ultrasound, Shanghai General Hospital, Shanghai Jiao Tong University School of Medicine, Shanghai, China
[2]Department of Ultrasonography, School of Medicine, The International Peace Maternity and Child Health Hospital, Shanghai Jiao Tong University, Shanghai, China

Received: 15 April 2024 / Accepted: 6 November 2024
Published online: 03 December 2024

References

1. Jiang YX, Liu H, Liu JB, et al. Breast tumor size assessment: comparison of conventional ultrasound and contrast-enhanced ultrasound[J]. Ultrasound Med Biol. 2007;33(12):1873–81.
2. Carraro DM, Elias EV, Andrade VP. Ductal carcinoma in situ of the breast: morphological and molecular features implicated in progression[J]. Biosci Rep. 2014;34(1). pii: e00090.
3. Vanbockstal M, Lambein K, Denys H, et al. Histopathological characterization of ductal carcinoma in situ (DCIS) of the breast according to HER2 amplification status and molecular subtype[J]. Virchows Arch. 2014;465(3):275–89.
4. Poulakaki N, Makris GM, Papanota AM, et al. Ki-67 expression as a factor predicting recurrence of ductal carcinoma in situ of the breast: a systematic review and meta-analysis[J]. Clin Breast Cancer. 2018;18(2):157–e1676.
5. Greenwood HI, Heller SL, Kim S, et al. Ductal carcinoma in situ of the breasts: review of MR imaging features[J]. Radiographics. 2013;33(6):1569–88.
6. Watanabe T, Yamaguchi T, Tsunoda H, et al. Ultrasound image classification of ductal carcinoma in situ (DCIS) of the breast: analysis of 705 DCIS lesions[J]. Ultrasound Med Biol. 2017;43(5):918–25.
7. Gunawardena DS, Burrows S, Taylor DB. Nonmass versus mass-like ultrasound patterns in ductal carcinoma in situ: is there an association with high-risk histology? [J]. Clin Radiol. 2020;75(2):140–7.
8. Moschetta M, Sardaro A, Nitti A, et al. Ultrasound evaluation of ductal carcinoma in situ of the breast[J]. J Ultrasound. 2022;25(1):41–5.
9. Evans A, Purdie CA, Jordan L, et al. Stiffness at shear wave elastography and patient presentation predicts upgrade at surgery following an ultrasound-guided core biopsy diagnosis of ductal carcinoma in situ[J]. Clin Radiol. 2016;71(11):1156–9.
10. Leong LC, Sim LS, Jara-Lazaro AR, et al. Ultrasound breast elastographic evaluation of Mass-Forming Ductal Carcinoma-in-situ with histological correlation - new findings for a Toothpaste Sign[J]. Asian Pac J Cancer Prev. 2016;17(5):2673–8.
11. Berg WA, Cosgrove DO, Doré CJ, et al. Shear-wave elastography improves the specificity of breast US: the BE1 multinational study of 939 masses[J]. Radiology. 2012;262(2):435–49.
12. Sanati S. Morphologic and molecular features of breast ductal carcinoma in situ [J]. Am J Pathol. 2019;189(5):946–55.
13. Hammond ME, Hayes DF, Dowsett M, et al. American Society of Clinical Oncology/College of American Pathologists guideline recommendations for immunohistochemical testing of estrogen and progesterone receptors in breast cancer[J]. J Clin Oncol. 2010;28(21):3543.
14. Poulakaki N, Makris GM, Battista MJ, et al. Hormonal receptor status, Ki-67 and HER2 expression: prognostic value in the recurrence of ductal carcinoma in situ of the breast? [J] Breast. 2016;25:57–61.
15. Hanna WM, Slodkowska E, Lu FI, et al. Comparative Analysis of Human Epidermal Growth Factor Receptor 2 testing in breast Cancer according to 2007 and 2013 American Society of Clinical Oncology/College of American Pathologists Guideline Recommendations[J]. J Clin Oncol. 2017;35(26):3039–45.
16. Harrison BT, Hwang ES, Partridge AH, et al. Variability in diagnostic threshold for comedo necrosis among breast pathologists: implications for patient eligibility for active surveillance trials of ductal carcinoma in situ[J]. Mod Pathol. 2019;32(9):1257–62.
17. Park JS, Park YM, Kim EK, et al. Sonographic findings of high-grade and non-high-grade ductal carcinoma in situ of the breast[J]. J Ultrasound Med. 2010;29(12):1687–97.
18. Schäfer FK, Hooley RJ, Ohlinger R, et al. ShearWave™ Elastography BE1 multinational breast study: additional SWE™ features support potential to downgrade BI-RADS®-3 lesions[J]. Ultraschall Med. 2013;34(3):254–9.
19. Hari S, Paul SB, Vidyasagar R, et al. Breast mass characterization using shear wave elastography and ultrasound[J]. DiagnInterv Imaging. 2018;99(11):699–707.
20. Chang JM, Moon WK, Cho N, et al. Clinical application of shear wave elastography (SWE) in the diagnosis of benign and malignant breast diseases[J]. Breast Cancer Res Treat. 2011;129(1):89–97.

21. Bae JS, Chang JM, Lee SH, et al. Prediction of invasive breast cancer using shear-wave elastography in patients with biopsy-confirmed ductal carcinoma in situ[J]. Eur Radiol. 2017;27(1):7–15.
22. Kim H, Lee J, Kang BJ, et al. What shear wave elastography parameter best differentiates breast cancer and predicts its histologic aggressiveness? [J]. Ultrasonography. 2021;40(2):265–73.
23. Lee EJ, Chang YW. Combination of quantitative parameters of Shear Wave Elastography and superb microvascular imaging to evaluate breast Masses[J]. Korean J Radiol. 2020;21(9):1045–54.
24. Evans A, Whelehan P, Thomson K, et al. Invasive breast cancer: relationship between shear-wave elastographic findings and histologic prognostic factors[J]. Radiology. 2012;263(3):673–7.
25. Evans A, Whelehan P, Thomson K, et al. Quantitative shear wave ultrasound elastography: initial experience in solid breast masses[J]. Breast Cancer Res. 2010;12(6):R104.
26. Meyer JS. Cell kinetics of histologic variants of in situ breast carcinoma[J]. Breast Cancer Res Treat. 1986;7:171–80.
27. Lagios MD, Margolin FR, Westdahl PR, et al. Mammographically detected duct carcinoma in situ. Frequency of local recurrence following tylectomy and prognostic effect of nuclear grade on local recurrence[J]. Cancer. 1989;63:618–24.
28. Yu PC, Lee YW, Chou FF, et al. Clustered microcalcifications of intermediate concern detected on digital mammography: ultrasound assessment[J]. Breast. 2011;20(6):495–500.
29. Nagashima T, Hashimoto H, Oshida K, et al. Ultrasound demonstration of Mammographically detected microcalcifications in patients with Ductal Carcinoma in situ of the Breast[J]. Breast Cancer. 2005;12(3):216–20.
30. YANG W T, TSE GM. Sonographic, mammographic, and histopathologic correlation of symptomatic ductal carcinoma in situ[J]. AJR Am J Roentgenol. 2004;182(1):101–10.
31. Niwińska A, Olszewski WP. The role of stromal immune microenvironment in the progression of ductal carcinoma in situ (DCIS) to invasive breast cancer. Breast Cancer Res. 2021;23(1):118.

Publisher's note